N. I. Elkalashy, M. Lehtonen, H. A. Darwish, A.-M. I. Taalab and M. A. Izzularab, DWT-Based Detection and Transient Power Direction-Based Location of High Impedance Faults Due to Leaning Trees in Unearthed MV Networks, The 7th International Conference on Power Systems Transients, IPST 2007, Lyon, France, June 4-7, 2007.

DWT-Based Detection and Transient Power Direction-Based Location of High Impedance Faults Due to Leaning Trees in Unearthed MV Networks

Nagy I. Elkalashy, *student, IEEE*, Matti Lehtonen, Hatem A. Darwish, *SMIEEE*, Abdel-Maksoud I. Taalab, *SMIEEE*, and Mohamed A. Izzularab

***Abstract*— Electrical faults due to leaning trees are common in Nordic Countries. This fault type has been studied in [1] and it was found that the initial transients in the electrical network due to the associated arc reignitions are behavioral traits. In this paper, these features are extracted using the discrete wavelet transform (DWT) to localize this fault event. Wireless sensors are considered for processing the DWTs on a residual voltage of different measuring nodes that are distributed in the network. Therefore, the fault detection is confirmed by numerous DWT processors over a wide area of the network. The detection security is also enhanced because the DWT is responded to a periodicity of the initial transients. The term for locating the faulty section is based on the polarity of a specific frequency band-power computed by multiplying the DWT detail coefficient of the residual current and voltage at each measuring node. The fault due to a leaning tree occurring at different locations in an unearthed 20 kV network is simulated by ATP/EMTP and the arc model is implemented using the universal arc representation. Test cases provide evidence of the efficacy of the proposed technique.**

***Index Terms*— Arc model, DWT, initial transients, residual current and voltage, wireless sensors.**

I. Introduction

SINCE the electrical network in the Nordic countries is exposed to leaning trees as a result of the large forest areas, it is worthwhile to study the detection of faults due to leaning trees. These faults are categorized as high impedance arcing faults due to the tree resistance (several hundred ohms) and associated arcs [1].

All research efforts directed towards the detection of high impedance faults help clarify their features and the practical considerations for their detection [2]-[9]. The features are extracted using filters such as the Fast Fourier Transform, Kalman Filter and Fractal and Wavelet Transforms [3]-[6]. Therefore, numerous detection algorithms have been motivated, depending on harmonic contents such as second order, third order, composite odd harmonics, even harmonics, nonharmonics, high frequency spectra and harmonic phase angle considerations [6]-[8]. Multiple algorithms can enhance the fault detection [9]. However, such techniques have not been applied for identifying faults due to a leaning tree.

The transients produced in electrical networks due to faults often depend on the neutral point treatments. They can be completely isolated from ground, earthed through impedance or solidly earthed at their neutral. In Nordic Countries, the neutral is commonly unearthed and compensated MV networks are increasingly being used [10]. The system used in this study is a 20 kV unearthed network. The directionality of the residual currents in the healthy and faulty branches with respect to a residual voltage is used as a protection function in unearthed systems [10]. However, the fault resistance associated with a leaning tree is very high, which limits its detection based on current amplitudes.

In this paper, the impact of the arc reignition periodicity on the residual waveforms is used to detect this fault. The initial transients in the vicinity of the current zero-crossing lead to fingerprints boosting the fault detection. These initial transients are localized based on the DWT detail coefficient of the residual voltages over a wide area of the network to reliably detect the fault. The wireless sensor concept is used for enhancing fault detection security and the location processes. At each measuring node, the DWT detail coefficients of the residual current and voltage are multiplied together. The summation is computed over a period of two power cycles to estimate the polarity of the frequency-band power. This polarity is found suitable for discriminating between the healthy and faulty branches at each node and the fault is therefore tracked. A practical 20 kV unearthed network is simulated in ATP/EMTP and ATPDraw is used as a graphical interface. The fault model is incorporated at different locations in the network and the associated arc is implemented using the universal arc representation.

II. Proposed Technique Principles

The proposed technique mainly depends on DWT and wireless sensor concept for the fault detection. In the following sub-sections, the wireless sensor concept and the detection technique are discussed.

A. Wireless sensor networks

The wireless sensor concept is a modern insight used for various tasks with the objective of saving time and expense. Wireless sensors are distributed throughout the electrical network. The

N. I. Elkalashy and M. Lehtonen are with Power Systems & High Voltage Engineering, Helsinki University of Technology (TKK), Finland.

H. A. Darwish, A-M. I. Taalab and M. A. Izzularab are with the Electrical Engineering Department, Faculty of Engineering, Shebin El-Kom 32511, Minoufiya Unversity, Egypt.

Presented at the International Conference on Power Systems Transients (IPST'07) in Lyon, France on June 4-7, 2007

electrical quantities are then regularity transmitted from the different measuring nodes and investigated for several purposes such as load monitoring, fault detection and location [11]-[13]. The availability of sensing devices, embedded processors, communication kits and power equipment enables the design of wireless sensors as depicted in the four major blocks in Fig. 1 [14]. New network protocols are necessary, including link, network, transport, and application layers to solve problems such as routing, addressing, clustering and synchronization. They have to be energy-efficient [14]. This paper will not explore these issues in more depth. The point is that the wireless concept is used for gathering data from different measuring nodes in the network.

B. Proposed Fault Detection Technique

The scenario of the fault detection and its location can be generalized using Fig. 2. At each measuring node, phase voltages and branch phase currents are measured. The corresponding residual currents and voltage are computed and they are extracted using DWT. The absolute sum of the residual voltage detail d3 coefficient over one cycle period of the power frequency is estimated for the fault detection purpose. A timer is used for determining the fault period and it can be implemented using a samples counter. Under certain circumstances controlled by wind speeds, the tree can move towards and away from the electrical network and the fault features can be repeated several times. Therefore, a counter can be added and used to determine a number of fault events.

In order to track the fault, the detail d3 of the residual voltage and current of each connected branch is multiplied to compute the residual power of the frequency range equal to the considered detail band. Using the sum over a period of two power cycles, the power direction in the form of its polarity is utilized for determining which branch leads to the fault point.

Once the fault features appear on the residual voltage details, the fault tracking process is considered and the protection response over a wide area of the network can be collected using wireless sensors. Although the fault features are extracted utilizing a high frequency band, the proposed technique performance can be transmitted at a lower sampling rate. Also, the communication process can be initiated at the fault occurrence using the voltage details.

III. SIMULATED SYSTEM

Figure 3 illustrates the single line diagram of an unearthed 20 kV, 5 feeder distribution network simulated using ATP/EMTP, in which the processing is created by ATPDraw [15]. The feeder lines are represented using the frequency dependent JMarti model consistent with the feeder configuration given in the Appendix. Although the network is isolated, it is grounded by the natural phases to ground capacitances. Therefore, the phase fault current is very low allowing service continuity [10].

An experiment was performed to measure the characteristics of faults due to leaning trees occurring in a 20 kV distribution network [1]. This fault type is modeled using two series parts: a dynamic arc model and a high resistance. For the considered case study, the resistance is equal to 140 kΩ [1]. Regarding the arc modeling, the most popular modeling rules depend upon thermal equilibrium that is adapted as following:

$$\frac{dg}{dt} = \frac{1}{\tau}(G - g) \tag{1}$$

$$G = \frac{|i|}{V_{arc}} \tag{2}$$

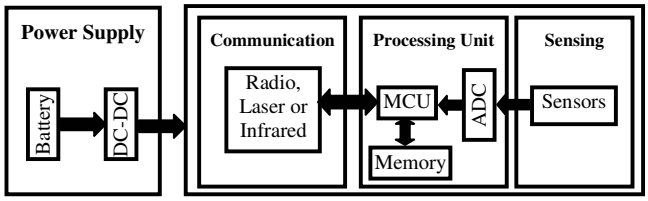

Fig. 1 Architecture of the sensor node system [14].

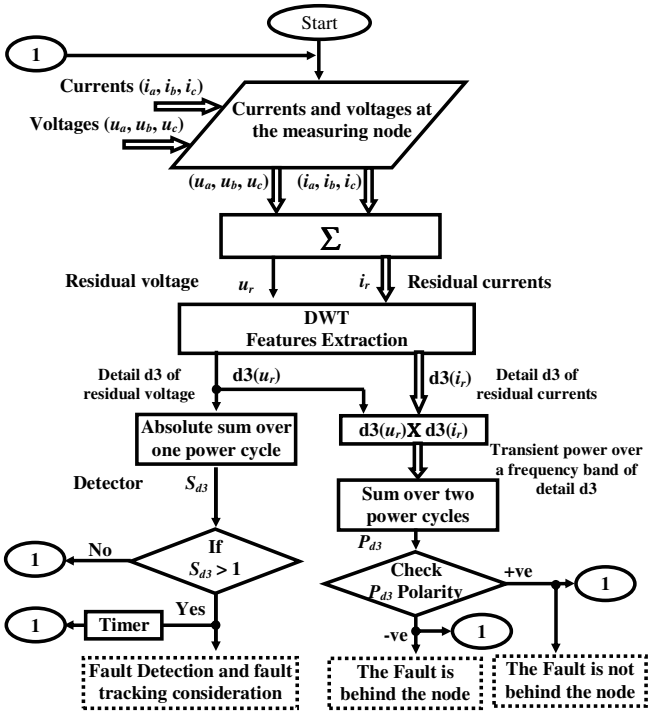

Fig. 2 The proposed detection technique.

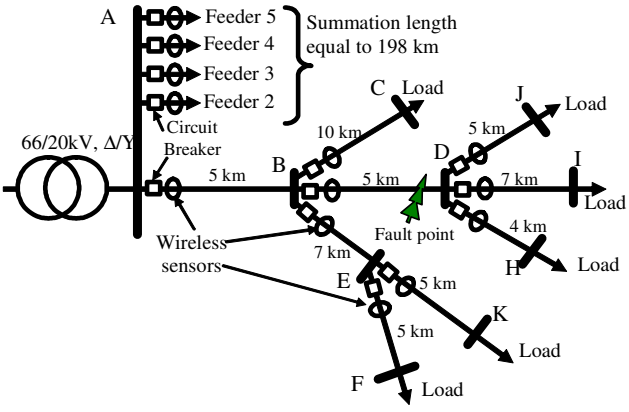

Fig. 3 Simulated system for a substation energized 251 km distribution network (5 feeders).

where g is the time-varying arc conductance, G is the stationary arc conductance, $|i|$ is the absolute value of the arc current, V_{arc} is a constant arc voltage parameter, and τ is the arc time constant. For representing the arc associated with this fault type, τ is changed to fit the new application as in [1]:

$$\tau = Ae^{Bg} \quad (3)$$

where A and B are constants. In [1], the parameters V_{arc}, A and B were experimentally found to be 2520V, 5.6E-7 and 395917, respectively. Considering the conductance at each zero crossing, the dielectric is represented by a variable resistance until the instant of reignition. It is represented using a ramp function of 0.5 MΩ/*ms* for a period of 1 *ms* after the zero-crossing and then 4 MΩ/ms until the reignition instant.

Considering the bilateral interaction between the EMTP power network and the transient analysis control system (TACS) field, the arcing equations (1), (2) and (3) are implemented using the universal arc representation [17]. The aforementioned MV network and the fault modeling are combined in a single arrangement, as shown in the ATPDraw circuit illustrated in the Appendix to describe the network behavior during this fault.

The best waveforms that can be analyzed for detecting high impedance ground faults occurring in unearthed distribution networks are the residual current and voltage waveforms. They are computed as:

$$i_r = i_a + i_b + i_c \quad (4)$$

$$u_r = u_a + u_b + u_c \quad (5)$$

where i_r and u_r are the residual current and voltage, respectively. i_a , i_b and i_c are the phase currents. u_a , u_b and u_c are the phase voltages. In order to investigate these residual waveforms during the fault, equations (4) and (5) are implemented in TACS for different locations over the network, as depicted in the ATPDraw circuit shown in the Appendix.

Referring to the simulated system shown in Fig. 3 with a fault occurring at the end of section BD, the corresponding residual waveforms are shown in Fig. 4 when this fault occurred at 26 *ms*. From the enlarged view shown in Fig. 4-a, it is obvious that it is the higher residual current amplitude that is measured in the faulty section and it is slightly reduced for the upstream section AB. The initial transients of the other sections that are healthy are also obvious at each zero-crossing. This is because of couplings between the network phases and the earth along with the feeder lengths. Fig. 4-b ensures that the effects of arc reignitions on the residual voltages are synchronized with the current zero-crossings.

Although there are perceptible differences in the performance of the residual current magnitudes during this fault that in principle can indicate the faulty section, it is not suitable to base the discrimination on such magnitudes directly. This is because they are very small (less than 100mA). However, the impacts of arc reignitions on the residual waveforms are obvious and can be exploited for detecting the fault. The most suitable signal processing technique for localizing these initial transients is DWT.

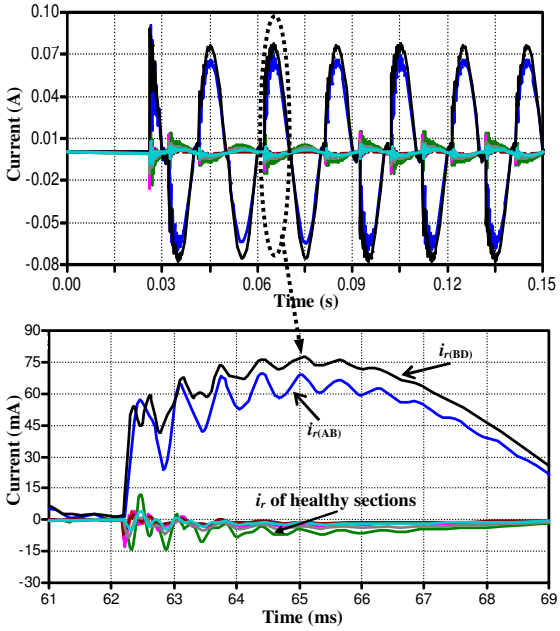

a- Enlarged view of residual current waveforms (i_r).

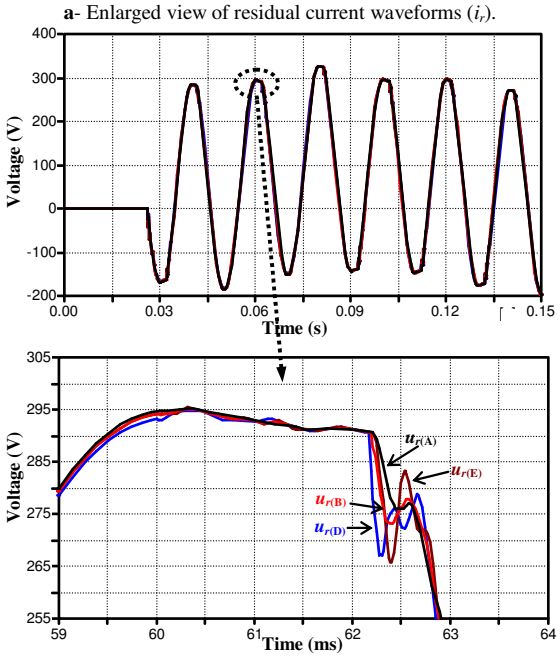

b- Enlarged view of residual voltage waveforms (u_r).

Fig. 4 The residual waveforms when the fault occurred in section BD.

IV. DWT-Based Fault Detection

Wavelets are families of functions generated from one single function, called the mother wavelet, by means of scaling and translating operations. The scaling operation is used to dilate and compress the mother wavelet to obtain the respective high and low frequency information of the function to be analyzed. Then the translation is used to obtain the time information. In this way a family of scaled and translated wavelets is created and it serves as the base for representing the function to be analyzed [18]. The DWT is in the form:

$$DWT_\psi f(m,k) = \frac{1}{\sqrt{a_o^m}} \sum_n x(n) \psi\left(\frac{k - nb_o a_o^m}{a_o^m}\right) \quad (6)$$

where $\psi(.)$ is the mother wavelet that is discretely dilated and translated by a_o^m and $nb_oa_o^m$, respectively. a_o and b_o are fixed values with $a_o>1$ and $b_o>0$. m and n are integers. In the case of the dyadic transform, which can be viewed as a special kind of DWT spectral analyzer, $a_o=2$ and $b_o=1$. DWT can be implemented using a multi-stage filter with down sampling of the output of the low-pass filter. The practical realization of the DWT is addressed in [19], where its experimental implementation was accomplished using DSP board (DSP1003) with a reduction of its lengthy execution time.

A. *Fault Detection*

Several wavelet families were tested to extract the fault features using the Wavelet toolbox incorporated into the MATLAB program [20]. Daubechies wavelet 14 (db14) is appropriate for localizing this fault. The Details d3 including the frequency band 12.5-6.25 kHz are investigated, in which the sampling frequency is 100 kHz. The sampling rate can be reduced to 50 or 25 kHz but the used coefficients will be details d2 or d1, respectively. However, they are not considered in order to avoid the experimental noise effect [19]. For the fault case depicted in Fig. 4, features of the residual voltages measured at different locations are analyzed as shown in Fig. 5. It is obvious that the initial transients due to arc reignitions are frequently localized. To find flags used as fault detectors, the absolute sum value of the residual voltage detail d3 over a period of the power frequency is computed in a discrete form at each measuring node, as in [21]:

$$S_{d3}(k) = \sum_{n=k-N+1}^{k} \left| d3\_u_r(n) \right| \qquad (7)$$

where $S_{d3}(k)$ means the detector in the discrete samples according to $d3\_u_r$, which is the detail level $d3$ of the residual voltage u_r. n is used for carrying out a sliding window covering 20 ms and N is a number of window samples. The performance of the detectors S_{d3} for different residual voltages is shown in Fig. 6, in which the residual voltage extractions are used rather than the current because the voltage details are the highest. All over the network, the detectors respond to the fault disturbance as shown in Fig. 6. This confirms the fault existence. Moreover, the considered detectors are high not only at the starting instant of the fault events but also during the fault period, which improves the protection security.

B. *Faulty Section Discrimination*

It should be noted that the aforementioned detectors can only localize the fault event; however, they cannot discriminate the faulty section. This shortcoming can be overcome with the aid of Fig. 7, which is an enlarged view of the details d3 of the residual voltage, Feeder 1, and the healthy feeders' residual currents at node A. It is recognizable that the details d3 of the residual voltage and currents of the healthy feeders are in-phase. However, the detail of the faulty feeder residual current is out of phase. This shifting can be supervised by multiplying the details of the residual voltage ($d3\_u_r$) and current ($d3\_i_r$). It can be considered to be the harmonic-band power over the frequency range 12.5-6.25 kHz. Then its polarity is estimated using summation over a period of two power frequency cycles as:

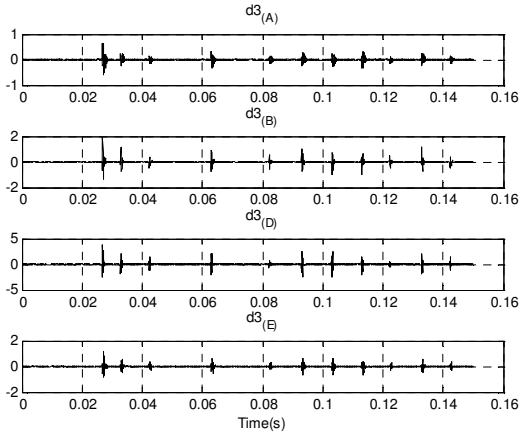

Fig. 5 Details d3 of the residual voltages at nodes A, B, D and E.

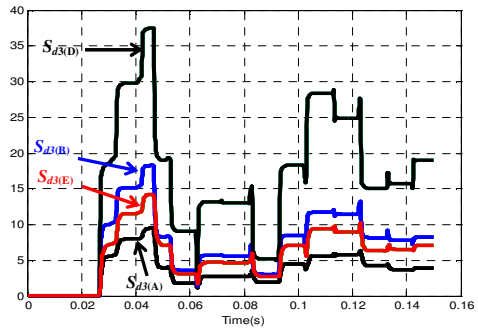

Fig. 6 The detector S_{d3} of the voltage details shown in Fig. 6-a.

$$P_{d3}(k) = \sum_{n=k-2N+1}^{k} \left| d3\_u_r(n) \times d3\_i_r(n) \right| \qquad (8)$$

where $P_{d3}(k)$ is used for the discrimination and its polarity is used to point out the fault point.

The discriminator performance is evident from Fig. 8, which illustrates P_{d3} at the measuring nodes A and B. Regarding node A shown in Fig. 8-a, the discriminator polarity is positive for healthy feeders and negative for faulty Feeder 1. For node B shown in Fig. 8-b, the discriminator polarity is positive for the healthy sections BC and BE but it is negative for the faulty section BD. When the discriminator polarities are checked at the measuring nodes D and E, they are found positive, ensuring the sections behind are healthy.

Another case was studied for a fault occurring at the end of section EF. The corresponding detectors S_{d3} of the residual voltages shown in Fig. 9 confirm the fault detection process. For determining the faulty section, the discriminator P_{d3} is computed for the branches at different nodes as depicted in Fig. 10, where this fault track is illustrated. Fig. 10-a shows that the fault track is in Feeder 1, Fig. 10-b points out that the track is then in section BE and Fig. 10-c illustrates that the track is then in section EF. Therefore, the fault route can be easily followed.

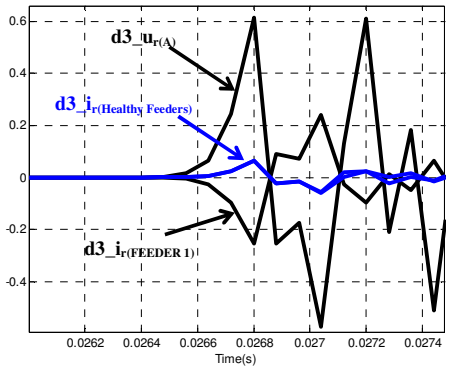

Fig. 7 Enlarged view of residual voltage and currents details at node A.

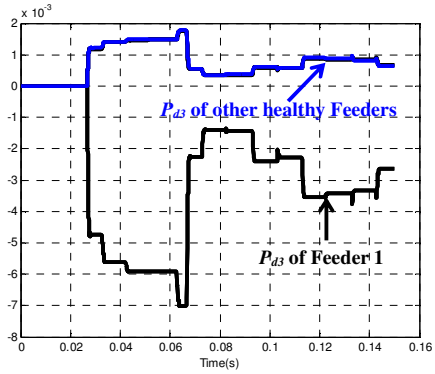

a- The discriminator P_{d3} at node A to determine the faulty feeder.

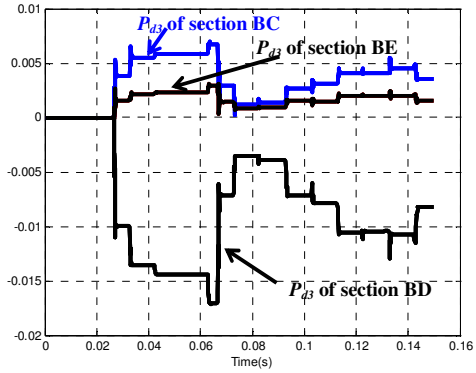

b- The discriminator P_{d3} at node B to determine the faulty section.

Fig. 8 The discriminator P_{d3} when the fault occurred in section BD.

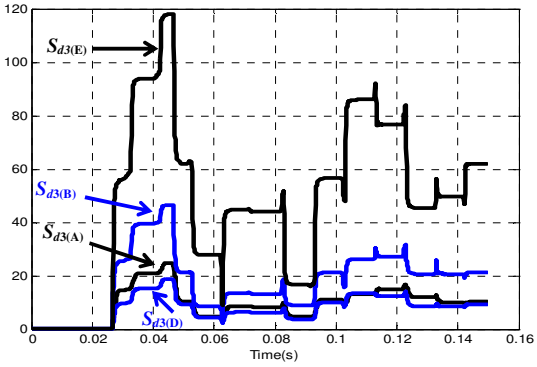

Fig. 9 The detector S_{di} when the fault occurred in section EF.

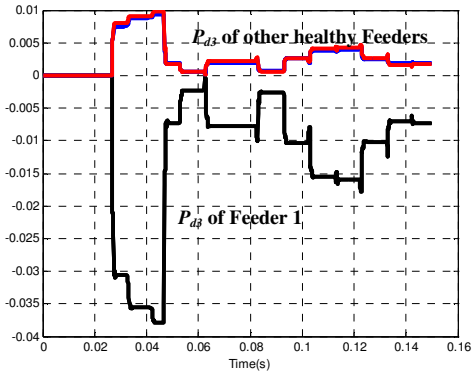

a- At node A.

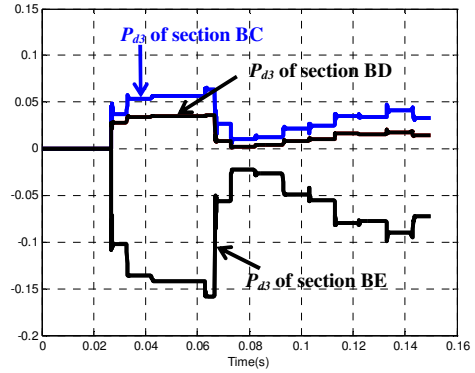

b- At node B.

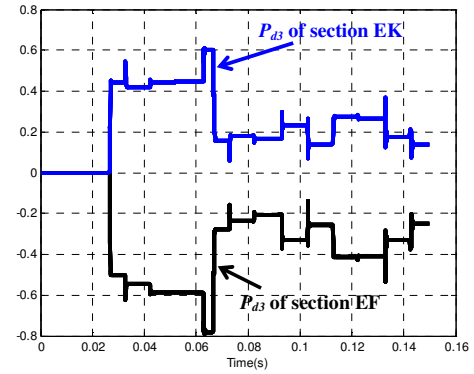

c- At node E.

Fig. 10 The discriminator P_{d3} when the fault occurred in section EF.

V. Conclusion

A novel technique for detecting a high impedance arcing fault due to a leaning tree has been introduced. The fault features have been extracted using DWT. The residual current and voltage waveforms have been computed at each measuring node in the electrical network. The periodicity of the arc reignitions gives a specific performance for the DWT with this fault type and the results enable fault detection. The fault track has been estimated using the polarities of the 12.5-6.25 kHz band-power computed by multiplying the detail d3 coefficients of the residual voltage and current. The proposed technique behavior has been investigated over a wide area of the simulated network utilizing the concept of allocated wireless sensors. Therefore, sensitive and secure detection of the faults due to leaning trees has been attained using DWT.

APPENDIX

Figure A illustrates the considered ATPDraw network. It contains the MV network shown in Fig. 3, the universal arc representation illustrated in Fig. 4 and the residual current and voltage waveforms described by (4) and (5), respectively. The feeders are represented using a frequency dependent JMarti model. Their configuration is shown in Fig. B.

ACKNOWLEDGMENT

The authors gratefully acknowledge the discussions with Mr. Abdelsallam Elhaffar and Mr. John Millar.

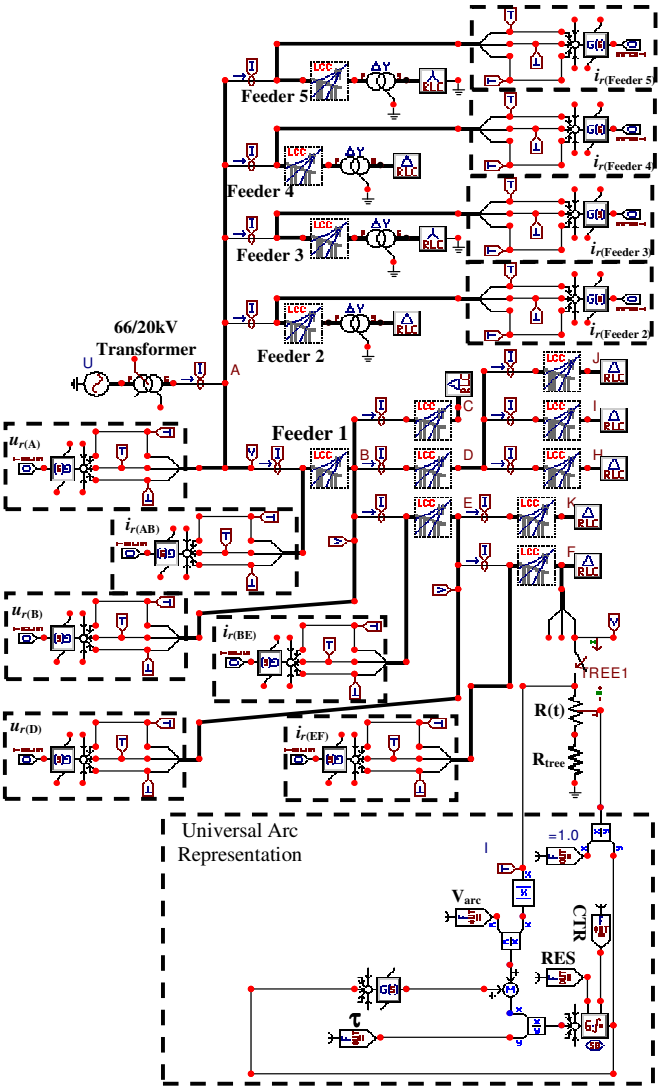

Fig. A The ATPDraw network.

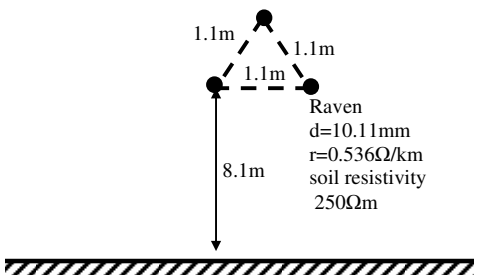

Fig. B The feeder configuration.

REFERENCES

[1] N. Elkalashy, M. Lehtonen, H. Darwish, M. Izzularab and A. Taalab "Modeling and Experimental Verification of a High Impedance Arcing Fault in MV Networks" Accepted at *IEEE Trans. Dielectric and Electrical Insulation*.

[2] J. Tengdin et. al. High Impedance Fault Detection Technology. Report of PSRC Working Group D15, March 1996.

[3] A. Girgis, W. Chang and E. Makram "Analysis of high-impedance fault generated signals using a Kalman filtering approach", *IEEE Trans. Power delivery*, vol. 5, no. 5, pp. 1714-1724, Oct. 1990.

[4] A. Mamishev, B. Russell and G. Benner "Analysis of High Impedance Faults Using Fractal Techniques", *IEEE Trans. Power delivery*, vol. 11, no. 1, pp. 435-440, Feb. 1996.

[5] A. Sedighi, M. Haghifam, O. Malik and M. Ghassemian "High Impedance Fault Detection Based on Wavelet Transform and Statistical Pattern Recognition", *IEEE Trans. Power delivery*, vol. 20, no. 4, pp. 1414-2421, Oct. 2005.

[6] D. Wai and X. Yibin "A Novel Technique for High Impedance Fault Identification", *IEEE Trans. Power delivery*, vol. 13, no. 3, pp. 738-744, July 1998.

[7] B. Russell and C. Benner "Arcing Fault Detection for Distribution Feeders: Security Assessment in Long Term Field Trials", *IEEE Trans. Power delivery*, vol. 10, no. 2, pp. 676-683, Apr. 1995.

[8] D. Jeeringes and J. Linders "Unique Aspects of Distribution System Harmonics due to High Impedance Ground Faults", *IEEE Trans. Power delivery*, vol. 5, no. 2, pp. 1086-1094, Apr. 1990.

[9] G. Benner and B. Russell "Practical High-Impedance Fault Detection on Distribution Feeders" *IEEE Trans. On Ind. Appl.*, vol. 33, no. 3, pp.635-640, May/June 1997.

[10] M. Lehtonen and T. Hakola "Neutral Earthing and Power System Protection. Earthing Solutions and Protective Relaying in Medium Voltage Distribution Networks", ABB Transmit Oy, FIN-65101 Vassa, Finland, 1996.

[11] M. Nordman and T. Korhonen "Design of a Concept and a Wireless ASIC Sensor for Locating Earth Faults in Unearthed Electrical Distribution Networks", *IEEE Trans. Power delivery*, vol. 21, no. 3, pp. 1074-1082, July 2006.

[12] R. Fernandes "Electrical Power Line and Substation Monitoring apparatus and systems" European Patent Applicat. 0314849, May 10, 1989.

[13] O. Vähämäki, K. Rautiainen and K. Kauhaniemi "Measurement of Quantities of Electric Line" Patent Applicat. WO0171367, Sep. 27, 2001.

[14] M. Vieira, C. Coelho, D. da Silva, J. da Mata "Survey on Wireless Sensor Network Devices" Emerging Technologies and Factory Automation, ETFA'03, 16-19 Sept. 2003, pp. 537–544.

[15] L. Prikler and H. Hoildalen, *ATPDraw users' manual*, SINTEF Energy Research AS, Norway, TR F5680, ISBN 82-594-2344-8, August 2002.

[16] M. Kizilcay and T. Pniok, "Digital Simulation of Fault Arcs in Power systems," *Europe Transaction on Electrical Power System, ETEP*, vol. 4, no. 3, pp. 55-59, Jan./Feb. 1991.

[17] H. Darwish and N. Elkalashy "Universal Arc Representation Using EMTP," *IEEE Trans. on Power Delivery*, Vol. 2, no. 2, pp 774-779, April 2005.

[18] M. Solanki, Y. Song, S. Potts and A. Perks "Transient protection of transmission line using wavelet transform" Seventh International Conference on Developments in Power System Protection,(IEE), pp. 299–302, 9-12 April 2001.

[19] H. A. Darwish, M. H. Farouk, A. I. Taalab, N. M. Mansour "Investigation of Real–Time Implementation of DSP-Based DWT for Power System Protection" IEEE/PES Transmission and Distribution Conference and Exposition, May 21-26, 2006, Dallas, Texas, USA.

[20] *Wavelet Toolbox for MATLAB*, Math Works 2005.

[21] J. Haung, C. Shen, S. Phoong and H. Chen "Robust Measure of Image Focus in the Wavelet Domain" International Symposium on Intelligent Signal Processing and Communication Systems, ISPACS2005, Dec. 13-16, 2006, Hong Kong.